Atmospheric Research 149 (2014) 88–95

Contents lists available at ScienceDirect

Atmospheric Research

journal homepage: www.elsevier.com/locate/atmos

Long-term trends in visibility and impacts of aerosol composition on visibility impairment in Baoji, China

S. Xiao [a,b,c], Q.Y. Wang [b], J.J. Cao [b,d,*], R.-J. Huang [e,f], W.D. Chen [a], Y.M. Han [b], H.M. Xu [b], S.X. Liu [b], Y.Q. Zhou [b], P. Wang [b], J.Q. Zhang [g], C.L. Zhan [g]

[a] Baoji Meteorological Bureau, Baoji 721006, China
[b] Key Laboratory of Aerosol Chemistry and Physics, SKLLQG, Institute of Earth Environment, Chinese Academy of Sciences, Xi'an 710075, China
[c] Climate Center of Shaanxi Meteorological Bureau, Xi'an 710014, China
[d] Institute of Global Environmental Change, Xi'an Jiaotong University, Xi'an 710049, China
[e] Laboratory of Atmospheric Chemistry, Paul Scherrer Institute (PSI), 5232 Villigen PSI, Switzerland
[f] Centre for Climate and Air Pollution Studies, Ryan Institute, National University of Ireland Galway, University Road, Galway, Ireland
[g] Environmental Science and Engineering College, Hubei Polytechnic University, Huangshi 435003, China

ARTICLE INFO

Article history:
Received 21 September 2013
Received in revised form 10 June 2014
Accepted 15 June 2014
Available online 20 June 2014

Keywords:
Visibility trend
Light extinction coefficient
$PM_{2.5}$ chemical composition
Source apportionment

ABSTRACT

Visibility impairment has become an important environmental issue receiving great attention from both the scientific community and the public. Long-term meteorological data from Baoji, China, were collected to investigate the trend in visibility change from 1980 to 2012. The 33-year average visual range is 12.0 km. The best 20% of the visibility observations in a calendar year shows a general decreasing trend from 1994 onwards, while the worst 20% exhibits a slight increasing trend from 1997 onwards. These results suggest the progressive degradation of air quality in Baoji in recent years. Intensive $PM_{2.5}$ measurements were conducted from March 2012 to February 2013 to determine the causes of visibility impairment. An analysis based on IMPROVE equation reveals that $PM_{2.5}$ organic matter (OM) contributes to 34.2% of the light extinction coefficient (b_{ext}) on an annual basis, followed by $(NH_4)_2SO_4$ (30.0%), NH_4NO_3 (20.1%), elemental carbon (9.2%) and soil dust (6.5%). The largest contributor to b_{ext} for the Worst 20% group is $(NH_4)_2SO_4$, and the contribution of NH_4NO_3 for the Worst 20% group increases by a factor of ~3 compared with the Best 20% group. Source apportionment using a positive matrix factorization receptor model indicates that secondary sulfate is the main source of $PM_{2.5}$ (23.0%), followed by fugitive dust (20.5%), coal combustion (19.9%), secondary nitrate (15.5%), biomass burning (14.3%) and motor vehicle emissions (6.8%). These quantitative results could be useful for policy makers to take effective measures to control the haze pollution in Baoji. Further, the results also are likely to be relevant for other mid-sized cities in China.

1. Introduction

Visibility impairment in urban environments has attracted considerable attention for scientific community worldwide (Chen and Xie, 2012; Wang et al., 2009; Zhang et al., 2010) and is also a concern for the public, especially those living in urban areas. Visibility degradation is more than an aesthetic issue; in fact, the atmospheric constituents responsible for the problem also affect the human and ecosystem health (Hyslop, 2009). Although natural emissions can be involved, emissions of anthropogenic pollutants are the major cause for degrading atmospheric visibility. Therefore, visibility has commonly been used as an indicator of air quality in urban areas (Watson, 2002). Previous studies (Huang et al., 2009; Thach et al., 2010) have used visibility degradation as a proxy for human exposure

* Corresponding author at: Key Laboratory of Aerosol Chemistry and Physics, SKLLQG, Institute of Earth Environment, Chinese Academy of Sciences, Xi'an 710075, China. Tel.: +86 29 8832 6488; fax: +86 29 8832 0456.
E-mail address: cao@loess.llqg.ac.cn (J.J. Cao).

http://dx.doi.org/10.1016/j.atmosres.2014.06.006
0169-8095/

to study the correlation between air quality and human mortality.

The degradation of visibility is a complicated issue because many factors can affect it simultaneously, including the concentrations, size distributions and composition of aerosol particles, which in turn are subject to the influence of different meteorological conditions (Cao et al., 2012a; Liu et al., 2013; Wang et al., 2013; Tao et al., 2014). Previous studies have shown that elevated concentrations of fine particles are the main cause of visibility impairment, mainly because fine particles scatter visible light more efficiently compared to coarse particles (Deng et al., 2008; Watson, 2002; Yang et al., 2007). In terms of the aerosol composition, sulfate, nitrate, organics and black carbon are the major species that impair visibility (Cao et al., 2012a; Wang et al., 2013; Yuan et al., 2006). Meteorological factors, especially relative humidity, wind speed and the depth of the planetary boundary layer (PBL) influence the concentrations and properties of aerosol particles and thus visibility (Wen and Yeh, 2010; Wu et al., 2005). In addition to the impacts of human activities, several natural phenomena, especially dust storms and fog, can also cause low visibility events (Kim et al., 2001; van Oldenborgh et al., 2010).

Even though particulate pollution has become one of the primary environmental concerns in China, most visibility studies have focused on provincial capitals or developed regions in eastern China (i.e., Che et al., 2009; Tao et al., 2009; Wang et al., 2013). In contrast, there has been relatively little attention paid to the problem in mid-sized cities. The measurement site in our study, Baoji (33°35′–35°06′N, 106°18′–108°03′E), is the second largest city of Shaanxi Province, with a population of over 0.75 million in the downtown area. Baoji is situated in north-central China on the northern bank of the Wei River (Fig. 1). Given that over 40% of the cities in China have a population and gross domestic product in size similar to Baoji (Wu, 2004), our results may have important implications for air pollution in mid-sized Chinese cities.

To better understand the visibility impairment problem in China, it is of particularly advantage to study the past and present visibility. Here, a long-term data set for visual range (VR) was used to investigate the changes in visibility in Baoji from 1980 to 2012. An intensive $PM_{2.5}$ measurement campaign was undertaken to investigate the potential causes of visibility impairment, and receptor modeling was used for source assessments.

2. Data and analysis methods

To investigate the long-term visibility trends in Baoji, China, daily records of VR as well as wind speed and relative humidity (RH) covering the period from 1980 to 2012 were obtained from the Baoji Meteorological Bureau. Well-trained observers measured the VR using reference objects, such as buildings and mountains, in different directions at known distances from the observer (Che et al., 2007). Daily optical light extinction coefficients (b_{ext}) are estimated from the well-known Koschmieder equation (Koschmieder, 1924):

$$b_{ext} = 3.912/VR \quad (1)$$

To characterize the impact of $PM_{2.5}$ on visibility impairment, an intensive sampling campaign was conducted on the rooftop (~10 m above ground level) of the Baoji Environmental Monitoring Station (see Fig. 1) from March 2012 to February 2013. Hourly $PM_{2.5}$ loadings were measured with an automatic Environmental Beta Attenuation Monitor (E-BAM, Met One Instruments, Inc., Grants Pass, OR, USA). Meanwhile, 24-hour integrated $PM_{2.5}$ samples were collected every 6 days from

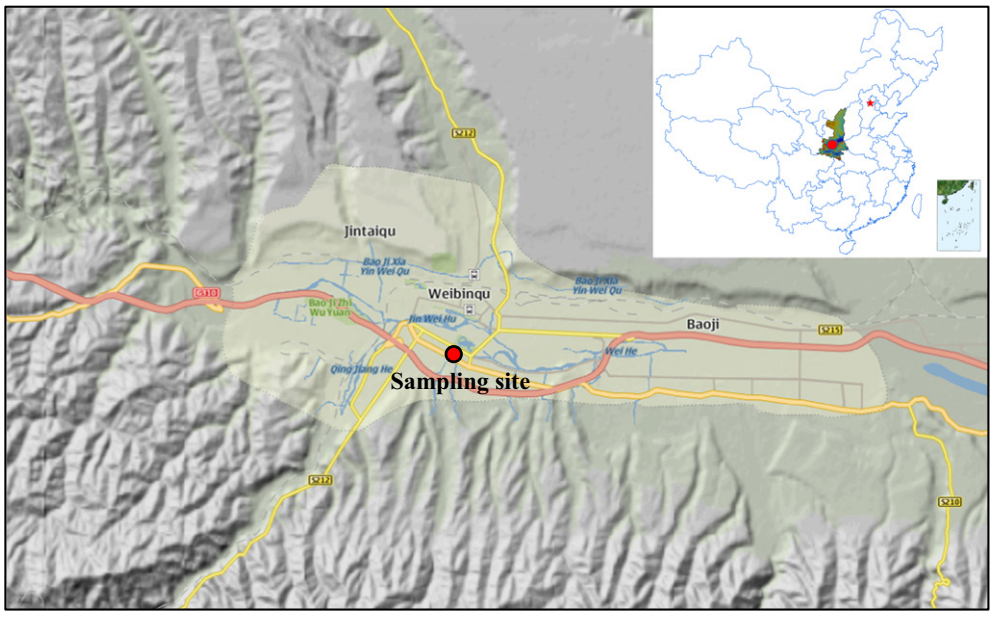

Fig. 1. Location of the Baoji sampling site.

10 a.m. to 10 a.m. the next day (local standard time) using two battery-powered mini-volume samplers (Airmetrics, Oregon, USA), which operated at a flow rate of 5 L min^{-1}.

One sampler was equipped with 47-mm quartz-fiber filters (QM/A; Whatman, Middlesex, UK) for water-soluble inorganic ions, organic carbon (OC) and elemental carbon (EC) analyses, while the other sampler used 47 mm Teflon® filters (Whatman Limited, Maidstone, UK) for elemental analysis. After sampling, the filter samples were stored in refrigerator at ~4 °C until chemical analysis to prevent evaporation of volatile components. Field blank filters were collected to account for the positive artifacts due to the condensation of gas-phase organic components onto the filter during and/or after sampling. A total of 59 pairs of $PM_{2.5}$ samples were collected. For discussion purposes, spring is defined here as March to May (15 pairs), summer June to August (15 pairs), autumn September to November (14 pairs) and winter December to the following February (15 pairs).

Seven elements (K, Ti, Mn, Fe, As, Br and Pb) were determined by energy-dispersive X-ray fluorescence (ED-XRF) spectrometry (Epsilon 5 ED-XRF, PANalytical B.V., Netherlands). The Epsilon 5 spectrometer uses a three-dimensional polarizing geometry with 11 secondary targets (i.e., CeO_2, CsI, Ag, Mo, Zr, KBr, Ge, Zn, Fe, Ti and Al) and one barkla target (Al_2O_3). This configuration provides a good signal-to-background ratio and low detection limits. The X-ray source is a side window X-ray tube with a gadolinium anode, operated at an accelerating voltage of 25–100 kV and a current of 0.5–24 mA (maximum power: 600 W). The characteristic X-ray radiation was detected using a liquid nitrogen-cooled, solid-state, germanium, PANalytical (PAN 32) detector.

Water-soluble inorganic ions were determined with a Dionex 600 ion chromatograph (Dionex Corp, Sunnyvale, CA). Cation (Na^+, K^+, Mg^{2+}, Ca^{2+} and NH_4^+) concentrations were separated using a CS12A column (Dionex Corp.) and 20 mM methane sulfonic acid as the eluent. Anions (SO_4^{2-}, NO_3^- and Cl^-) were separated with an ASII-HC column (Dionex Corp.) and an eluent of 20 mM KOH. The limits of detection were less than 0.05 mg L^{-1} for both anions and cations. Standard Reference Materials produced by the National Research Center for Certified Reference Materials (China) were analyzed for quality control and assurance purposes. Blank values were subtracted from sample concentrations.

Carbonaceous species (OC and EC) were analyzed by a DRI (Model 2001) Thermal/Optical Carbon Analyzer (Atmoslytic Inc., Calabasa, CA, USA). The method produces data for (A) four OC fractions (OC1, OC2, OC3 and OC4 in a helium atmosphere at 140 °C, 280 °C, 480 °C and 580 °C, respectively); (B) a pyrolyzed carbon fraction (OP, determined when reflected laser light attained its original intensity after oxygen was added to the combustion atmosphere); and (C) three EC fractions (EC1, EC2 and EC3 in a 2% oxygen/98 % helium atmosphere at 580 °C, 740 °C and 840 °C, respectively). The IMPROVE A protocol defines OC as OC1 + OC2 + OC3 + OC4 + OP and EC as EC1 + EC2 + EC3 − OP. The analyzer was calibrated with known quantities of CH_4 daily. Replicate analyses were performed for one sample in every ten samples. Field blank samples were also analyzed, and the sample results were corrected for the field blanks. More detailed descriptions of Quality Assurance/Quality Control (QA/QC) procedures can be found in Cao et al. (2003).

3. Results and discussion

3.1. Long-term trend in visibility

The mean and median VRs in Baoji are relatively stable from 1980 to 2012 (Fig. 2). The 33-year average VR is 12.0 km, with the maximum annual average occurring in 1995 (13.9 km) and the minimum in 1985 (10.3 km). The 33-year average VR in Baoji is higher than that at Chinese megacities Guangzhou (10.8 km), Beijing (10.7 km), Shanghai (8.6 km) (Chang et al., 2009) or Chengdu (8.5 km) (Wang et al., 2013), but lower than that at Nanjing (16.5 km) and Hangzhou (15.1 km) (Gao et al., 2011).

The 50th percentile (50%) of the observations in a calendar year, the 20th percentile with the lowest VRs (Worst 20%) and the 20th percentile with the highest VRs (Best 20%) are used here as indicators of "median visibility," "poor visibility" and "good visibility," respectively, based on the U.S. Regional Haze Rules (Environmental Protection Agency, 1999). As shown in Fig. 2, the Worst 20%, 50% and the Best 20% exhibit similar fluctuations during the study period, with 33-year average values of 4.2, 12.0 and 20.1 km, respectively. For the Worst 20% group, the highest VR is 6.6 km in 2012, and the lowest is 3.1 km in 1997. For the 50% VR group, the highest value is 15.0 km in 2005, and the lowest value is 10.0 km in 1985. For the Best 20% group, the highest VR is 23.2 km in 1989, and the lowest is 16.9 km in 2011. It should be noted that although there is some fluctuation for certain years, the Best 20% of the annual observations show a general decreasing trend of ~2.0 km/decade from 1994 onwards, while the Worst 20% exhibits a slight increasing tendency of ~1.0 km/decade from 1997 onwards. The fluctuation could be associated with the combination effects of $PM_{2.5}$ and meteorological conditions.

Fig. 3a and b show the correlations of the yearly averaged VR with wind speed and RH, respectively. The correlation coefficients show that visual range increase with wind speed, most likely due to enhanced dilution of air pollutants

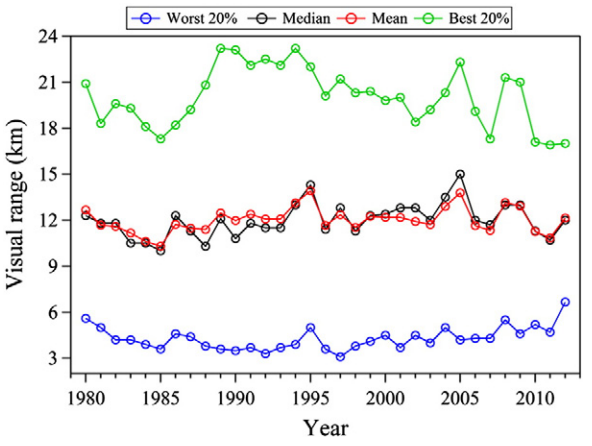

Fig. 2. The 33-year trend of annual average visual range as well as the Best 20%, 50% and the Worst 20% of the annual visual range observed from 1980 to 2012 in Baoji, China.

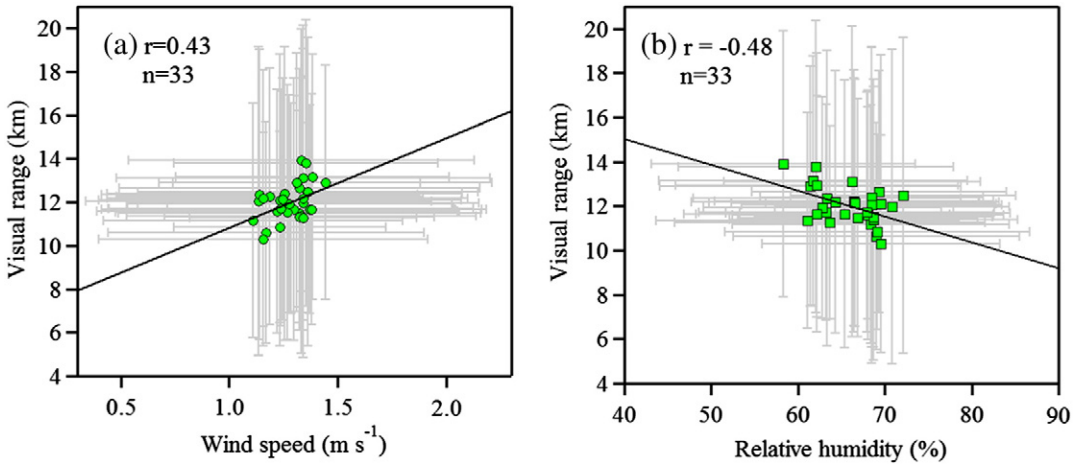

Fig. 3. Scatter plots of the annual average visual ranges versus (a) wind speed and (b) relative humidity from 1980 to 2012. Vertical and horizontal error bars represent the standard deviations. Solid lines are the linear regression curves.

under high wind speeds. In contrast, the VR decrease with the increase of RH, most likely because higher RH promotes the growth of hygroscopic particles (e.g., sulfates and nitrates) into large sizes that scatter more light (Watson, 2002).

3.2. Correlation of visual range with $PM_{2.5}$ mass loadings

Fig. 4 shows the daily VR as a function of $PM_{2.5}$ mass concentration during the 1-year intensive study period from March 2012 to February 2013. The data points are color coded for RH and size coded for wind speed. It can be seen that the VR is exponentially related to $PM_{2.5}$ mass, with a correlation coefficient of 0.73. The China Meteorological Administration (2010) defines haze based on two meteorological variables: (i) the atmospheric horizontal visibility is less than 10 km, and (ii) the RH is lower than 80%. In terms of the exponential fit, the threshold of $PM_{2.5}$ mass concentration for the occurrence of haze at Baoji is equivalent to ~112 μg m^{-3}. In other words, when $PM_{2.5}$ mass concentrations are above this threshold value, the visibility in Baoji is typically low. Such analysis therefore provides a scientifically derived $PM_{2.5}$ standard that the local government may use to improve the visibility. It should be noted that this threshold value is 30% higher than the value of 88 μg m^{-3} in Xi'an (Cao et al., 2012a), but comparable to the value of 110 μg m^{-3} in Beijing (Zhao et al., 2011). Differences in these local threshold values could be attributed to the different chemical composition of $PM_{2.5}$ in these three cities. Fig. 4 also shows that in general the VR is negatively correlated with RH and positively correlated with the wind speeds during the 2012–2013 intensive campaign period, consistent with the conclusion made from the long-term observations (1980–2012, see Fig. 3).

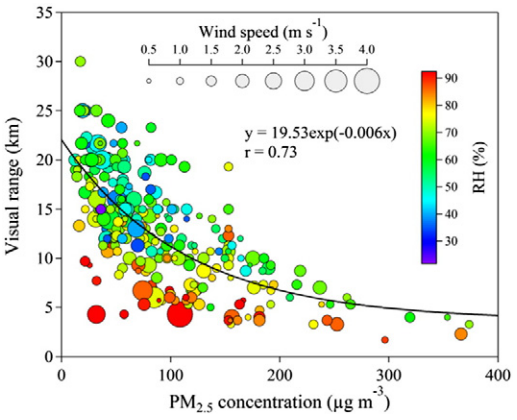

Fig. 4. Visual range as a function of $PM_{2.5}$ mass concentration in Baoji from March 2012 to February 2013. Data points are color coded for relative humidity (RH) and size coded for wind speed. The exponential curve is fitted between visual range and $PM_{2.5}$ mass.

The correlation matrix in Table 1 illustrates that the VR is negatively correlated with the concentrations of secondary inorganic ions, including SO_4^{2-} ($r = -0.68$), NO_3^- ($r = -0.6$) and NH_4^+ ($r = -0.7$). Although the VR is also negatively related to Cl^-, Na^+, K^+, Ca^{2+}, OC and EC, the correlation coefficients are much lower, in the range of −0.5 to −0.4. In addition, NH_4^+ is strongly correlated with SO_4^{2-} (0.94) and NO_3^- (0.96), suggesting that these three major ions are in the form of ammonium sulfate and ammonium nitrate. In urban air, the secondary inorganic aerosols are formed through the oxidation of their precursors SO_2 and NOx which are mainly emitted from coal burning and vehicle exhausts. Thus, it's important to control emissions from these two sources.

3.3. Influences of chemical components on light extinction coefficients

The degradation of visibility occurs as a result of the scattering and absorption of light by particles and gases in the

atmosphere. In this study, aerosol light extinction coefficient (b_{ext} in Mm^{-1}) is calculated from the IMPROVE equation:

$$b_{ext} = 3 \times f(RH) \times [\text{ammonium sulfate}] + 3 \times f(RH) \times [\text{ammonium nitrate}] + 4 \times [\text{organic matter}] + 1 \times [\text{soil dust}] + 10 \times [EC] + 1.7 \times f(RH) \times [\text{sea salt}] + 0.6 \times [\text{coarse mass}] + \text{Rayleigh Scattering(site specific)} \quad (2)$$

where the quantities in brackets [X] represent the concentrations of the $PM_{2.5}$ components in $\mu g\ m^{-3}$. A RH growth function f(RH) indicates the extent of scattering efficiencies increase for sulfate and nitrate as they absorb liquid water. The f(RH) curve from Malm and Day (2001) is used for this study. The IMPROVE equation has been proven to be a useful tool for assessing the impact of specific types of aerosols on visibility (e.g., Kim et al., 2006; Tao et al., 2009).

Based on the ion-balance calculation (not shown), the SO_4^{2-} and NO_3^- can be completely neutralized by NH_4^+ to form $(NH_4)_2SO_4$ and NH_4NO_3. Thus, the concentrations of $(NH_4)_2SO_4$ and NH_4NO_3 are calculated by multiplying $[SO_4^{2-}]$ and $[NO_3^-]$ by a factor of 1.40 and 1.29, respectively. The organic matter (OM) and soil dust fractions are estimated from 1.6 × [OC] (Turpin and Lim, 2001) and [Fe]/0.035 (Taylor and McLennan, 1985), respectively. As Baoji is an inland city, the concentration of sea salt could be negligible compared to the major composition and was set as zero for simplified purpose. Moreover, the contributions of coarse mass and Rayleigh scattering to b_{ext} have been found to be negligible (Cao et al., 2012a; Cheung et al., 2005), and therefore, these factors also are excluded from the analysis.

As shown in Fig. 5, the reconstructed chemical b_{ext} correlates strongly with the optical b_{ext} estimated from the Koschmieder equation (Koschmieder, 1924). The slope of a least-squares linear regression is 1.09 and r = 0.78. These results suggest that the IMPROVE algorithm can provide reasonable estimates for chemical b_{ext} in Baoji under ambient conditions. Nevertheless, at high b_{ext} range, the discrepancies between optical b_{ext} and chemical b_{ext} are larger, which could be associated with the larger uncertainties from the naked-eye observations of lower VR although the observers are well-trained. The uncertainty in f(RH) may also lead to the deviation in estimating the chemical b_{ext}. Table 2 shows that the annual average (± standard deviation) chemical b_{ext} is 494 ± 314.8 Mm^{-1}, with the highest value occurring in winter (754 Mm^{-1}) followed by autumn (417 Mm^{-1}), summer (402 Mm^{-1}) and spring (397 Mm^{-1}). The annual average chemical b_{ext} at Baoji is higher than what is measured at Jinan (292 Mm^{-1}, Yang et al., 2007) or Guangzhou (367 Mm^{-1}, Jung et al., 2009), but much lower than that measured at Xi'an (912 Mm^{-1}, Cao et al., 2012a) and Chengdu (900 Mm^{-1}, Wang et al., 2013).

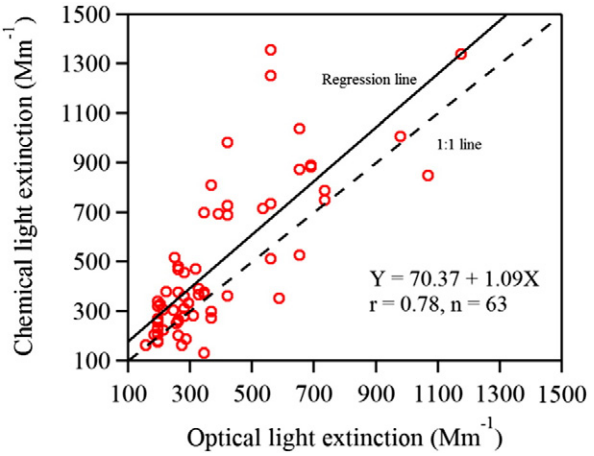

Fig. 5. Scatter plots of the chemical light extinction coefficient (b_{ext}) based on the IMPROVE equation versus optical light extinction coefficient (b_{ext}) estimated from the Koschmieder equation.

On average, OM is the largest contributor to the light extinction coefficient, accounting for 34.2% of chemical b_{ext}. The fractional contribution of OM to b_{ext} is the highest in winter (41.5%), followed by autumn (35.2%), spring (35.1%) and summer (18.8%). The second most important contributor to b_{ext} is $(NH_4)_2SO_4$ with an annual average of 30.0%. The highest contribution (48.7%) from $(NH_4)_2SO_4$ to b_{ext} is found in summer, presumably due to the high concentrations of SO_4^{2-} and high RH compared with the other seasons. The influence of NH_4NO_3 is also important throughout the year, with seasonal contributions of 16.7–21.8%. Particle light absorption by EC contributes to 9.2% of b_{ext}, and the remaining 6.5% of b_{ext} is attributed to soil dust.

Previous studies have shown that the relative influences of chemical species on b_{ext} vary with locations. For urban

Table 1
Correlations between $PM_{2.5}$ chemical components and visual range (VR) ($r > 0.8$ are shown underlined and in bold type).

	VR	SO_4^{2-}	NO_3^-	Cl^-	NH_4^+	Na^+	K^+	Ca^{2+}	OC	EC
VR	1									
SO_4^{2-}	−0.68	1								
NO_3^-	−0.60	**0.84**	1							
Cl^-	−0.45	0.42	0.62	1						
NH_4^+	−0.70	**0.94**	**0.96**	0.61	1					
Na^+	−0.40	0.42	0.37	0.54	0.43	1				
K^+	−0.50	0.75	**0.88**	0.67	**0.86**	0.34	1			
Ca^{2+}	−0.40	0.20	0.23	0.43	0.25	0.44	0.16	1		
OC	−0.45	0.45	0.66	**0.88**	0.66	0.52	0.65	0.46	1	
EC	−0.43	0.45	0.59	**0.81**	0.61	0.47	0.58	0.40	0.79	1

OC: organic carbon; EC: elemental carbon.

Table 2
Light extinction (b_{ext} in Mm^{-1}) budgets for $PM_{2.5}$ components by season.

Season	$(NH_4)_2SO_4$	NH_4NO_3	OM	EC	Soil dust	Total b_{ext}
Spring	109.3 ± 104.2	66.1 ± 74.2	139.2 ± 56.8	34.8 ± 16.2	47.2 ± 44.1	396.6 ± 208.3
% of b_{ext}	27.6	16.7	35.1	8.8	11.9	
Summer	195.8 ± 176.3	80.9 ± 95.2	75.5 ± 11.2	32.5 ± 11.7	17.1 ± 4.1	401.9 ± 287.6
% of b_{ext}	48.7	20.1	18.8	8.1	4.2	
Autumn	103.1 ± 73.6	83.7 ± 67.7	146.6 ± 86.1	51.4 ± 30.4	32.2 ± 23.8	417.0 ± 220.2
% of b_{ext}	24.7	20.1	35.2	12.3	7.7	
Winter	181.9 ± 129.0	164.2 ± 149.7	313.0 ± 121.1	62.4 ± 21.5	32.5 ± 14.9	753.9 ± 376.7
% of b_{ext}	24.1	21.8	41.5	8.3	4.3	
Annual	148.3 ± 130.8	99.0 ± 107.1	169.0 ± 118.2	45.2 ± 23.9	32.2 ± 27.8	493.6 ± 314.8
% of b_{ext}	30.0	20.1	34.2	9.2	6.5	

sites in China, Cao et al. (2012a), Yang et al. (2007) and Jung et al. (2009) found that $(NH_4)_2SO_4$ is the largest contributor to b_{ext}, accounting for 37–41% of b_{ext} in Xi'an, Jinan and Guangzhou, respectively, followed by OM (22–27%). For non-urban sites in USA, Malm and Day (2000) reported that OM contributes to ~35% of b_{ext} in the western USA, while sulfate contributes to ~60–70% of b_{ext} in the eastern USA. These large differences can be attributed to the variability in the major chemical species responsible for light scattering at different sites as well as to the effects of the ambient RH on particle growth.

To further investigate the contributions of chemical species to b_{ext}, budgets for the $PM_{2.5}$ components during the Best 20% and Worst 20% visibility days are calculated. As shown in Fig. 6, for the Best 20% group, OM (39.9%) have the largest effect on b_{ext}, followed by $(NH_4)_2SO_4$ (29.5%), EC (12.1%), soil dust (9.7%) and NH_4NO_3 (8.7%). In contrast, for the Worst 20% group, $(NH_4)_2SO_4$ (32.0%) have the largest effect on b_{ext}, followed by OM (30.6%), NH_4NO_3 (27.3%), EC (7.1%) and soil dust (3.0%). Even though the contribution of $(NH_4)_2SO_4$ have the largest effect on b_{ext} under the worst VR conditions, it should be noted that the contribution of NH_4NO_3 increased by a factor of ~3 from the Best 20% to Worst 20% group. This indicates that emissions from fossil fuel combustion play an important role in visibility degradation on Worst 20% days.

3.4. Mass balance and source apportionment of $PM_{2.5}$

More than 90% of the $PM_{2.5}$ mass during the four seasons is constituted by the following six components (Fig. 7): the major water-soluble inorganic ions (SO_4^{2-}, NO_3^- and NH_4^+), OM, EC and soil dust. On an annual basis, the most abundant components of $PM_{2.5}$ are OM (28.0%) and soil dust (27.0%), consistent with the results from fourteen Chinese cities reported by Cao et al. (2012b). During spring, soil dust constitutes the largest fraction of $PM_{2.5}$, accounting for 42.3% of the mass, followed by OM (27.1%) and SO_4^{2-} (13.6%). In summer, SO_4^{2-} is the largest contributor, accounting for 28.5% of the $PM_{2.5}$ mass, followed by OM (21.1%), soil dust (20.9%), NO_3^- (11.0%), NH_4^+ (6.9%) and EC (4.4%). During autumn, soil dust (28.2%) and OM (28.0%) are the main components of $PM_{2.5}$, followed by SO_4^{2-} (14.6%) and NO_3^- (12.1%). Finally, in winter, OM is the largest contributor to $PM_{2.5}$, followed by soil dust (16.6%), SO_4^{2-} (15.5%), NO_3^- (13.6%), NH_4^+ (7.1%) and EC (3.6%).

A positive matrix factorization (PMF) model, which is widely used in source apportionment (Cao et al., 2012a; Chen et al., 2010), is used to estimate the relative contribution of aerosol sources that cause the visibility impairment. The principles of PMF are described in detail elsewhere (Paatero and Tapper, 1994). For the present study, seven elements (K, Ti, Mn, Fe, As, Br and Pb), secondary inorganic ions (NO_3^-,

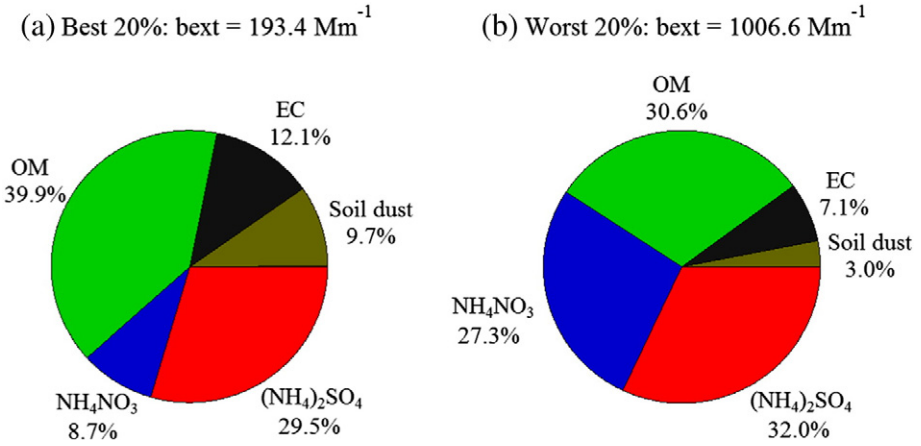

Fig. 6. Relative source contributions to chemical light extinction for the Best 20% and the Worst 20% of the annual visual range in Baoji between March 2012 and February 2013.

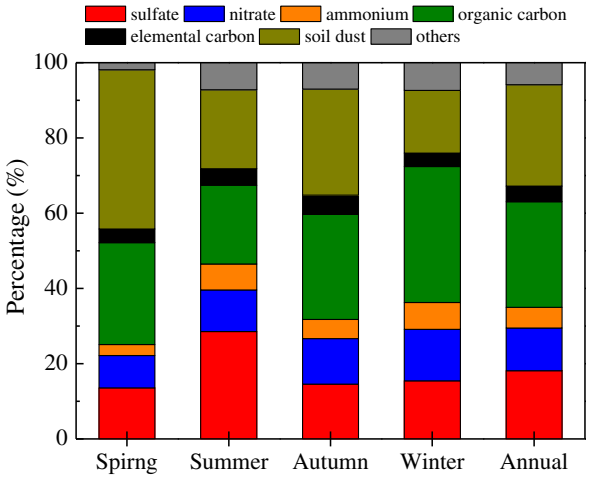

Fig. 7. Mass balances of chemical species in $PM_{2.5}$ from Baoji for the four seasons and the entire year (March 2012–February 2013).

SO_4^{2-} and NH_4^+) and carbonaceous species (OC and EC) are used as the model input. The resulting PMF factor profiles are shown in Fig. 8. Linear regression analysis is then used to estimate the contributions of major sources/factors to the $PM_{2.5}$ mass concentrations. The average source contributions calculated are presented in Fig. 9.

Factor 1 is characterized with high load of SO_4^{2-} and NH_4^+, which is associated with secondary sulfate and accounts for 23.0% of the $PM_{2.5}$ mass. Factor 2 has high loading of NO_3^- and NH_4^+, which is assigned to secondary nitrate. This factor constitutes 15.5% of the $PM_{2.5}$ mass. Factor 3 is characterized with high contents of As, Pb, EC and Mn, most likely associated with coal combustion. This factor accounts for 19.9% of $PM_{2.5}$ mass. Factor 4 has high loadings of Br, EC and OC and is characterized with motor vehicular emissions (Kim and Hopke, 2004). This factor accounts for 6.8% of $PM_{2.5}$ mass. Factor 5, biomass burning, is characterized with high concentrations of K and OC (Xie et al., 2008), accounting for 14.3% of $PM_{2.5}$ mass. Factor 6 is dominated by crustal elements Ti, Mn and Fe. This factor represents fugitive dust derived mainly from unpaved road dust resuspension and construction activities, which accounts for 20.5% of $PM_{2.5}$ mass.

4. Conclusions

Analyses of a long-term (1980–2012) data set of the visibility in Baoji show that the 33-year average visual range is 12.0 km. Although there is some fluctuation for certain years, the Best 20% of the visibility observations for each year shows a general decreasing trend of ~2.0 km/decade from 1994 onwards, while the Worst 20% of the annual observations exhibits a slight increasing tendency of ~1.0 km/decade from 1997 onwards. This indicates that air pollution in Baoji is getting worse in recent years.

Elevated $PM_{2.5}$ mass concentrations are associated with visibility lower than 10 km, and a $PM_{2.5}$ threshold value of 112 μg m^{-3} is empirically derived from the relationship between the daily visibility and the $PM_{2.5}$ mass concentration (that is, low visibility is observed when daily $PM_{2.5}$ mass

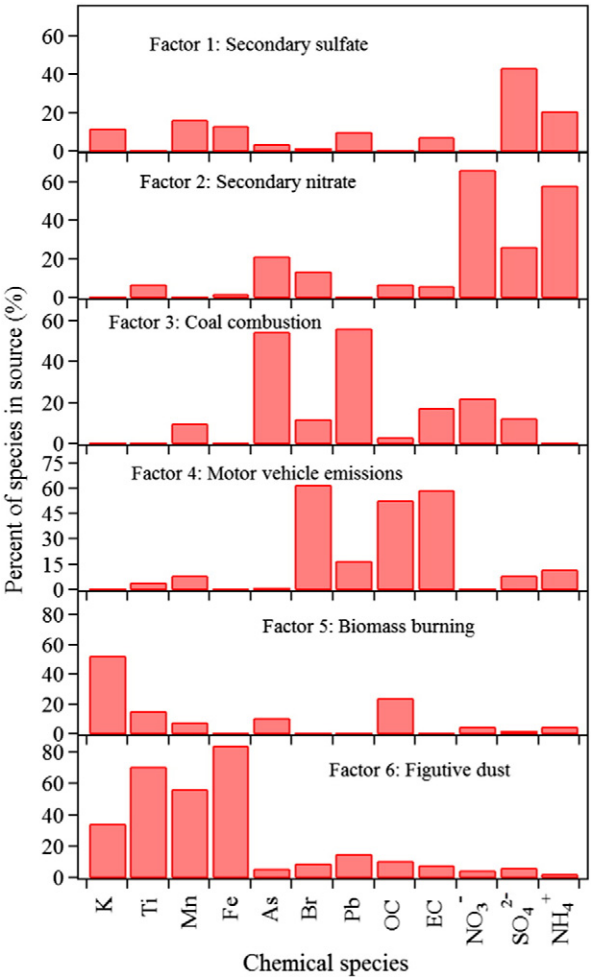

Fig. 8. Source profiles for the six sources identified by the positive matrix factorization (PMF) model during the intensive sampling period in Baoji. The *Y*-axes represent the percentage that each source contributes to individual species.

loading exceeds 112 μg m^{-3}). Based on a method established by the IMPROVE program, organic matter (OM) is found to be the largest contributor to visibility impairment overall, accounting for 34.2% of b_{ext}, followed by $(NH_4)_2SO_4$ (30.0%), NH_4NO_3 (20.1%), EC (9.2%) and soil dust (6.5%). For the Best 20% of the visibility for each year, OM (39.9%) is the largest contributor to b_{ext}, followed by $(NH_4)_2SO_4$ (29.5%), EC (12.1%), soil dust (9.7%) and NH_4NO_3 (8.7%). In contrast, for the Worst 20% of the visibility, $(NH_4)_2SO_4$ (32.0%) is the largest contributor to b_{ext}, followed by OM (30.6%), NH_4NO_3 (27.3%), EC (7.1%) and soil dust (3.0%). $PM_{2.5}$ mass balance analysis indicates that OM (28.0%) and soil dust (27.0%) are the most abundant components of the $PM_{2.5}$ mass overall. The PMF receptor model indicates that secondary sulfate is the main contributor to $PM_{2.5}$ mass, accounting for 23.0% of the $PM_{2.5}$ mass loading, followed by fugitive dust (20.5%), coal combustion (19.9%), secondary nitrate (15.5%), biomass burning (14.3%) and motor vehicle emissions. Our results quantify the sources responsible for visibility impairment in Baoji and therefore provide a scientific suggestion for the

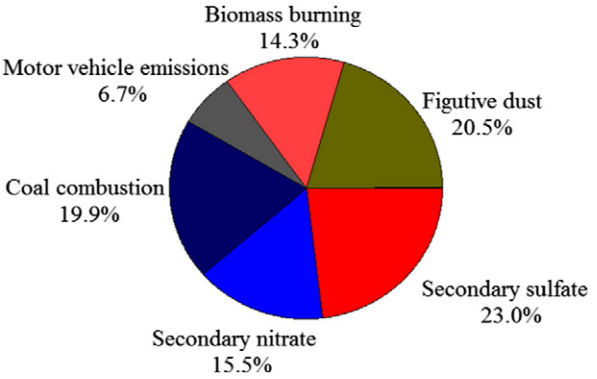

Fig. 9. Average source contribution for each PMF source factor to $PM_{2.5}$ mass concentration in Baoji (March 2012–February 2013).

development of practical pollution control measures for the local policy makers.

Acknowledgments

This study was supported by the project from "Strategic Priority Research Program" of the Chinese Academy of Science (XDA05100401), Meteorological Innovative Research Project of Baoji Meteorological Bureau (No.T2012-01), Shaanxi Government (2012KTZB03-01 and 2011KTCQ03-04) and Doctoral Program of Shaanxi Meteorological Bureau (2013B-1).

References

Cao, J.J., Lee, S.C., Ho, K.F., Zhang, X.Y., Zou, S.C., Fung, K., Chow, J.C., Watson, J.G., 2003. Characteristics of carbonaceous aerosol in Pearl River Delta Region, China during 2001 winter period. Atmos. Environ. 37, 1451–1460.

Cao, J.J., Wang, Q.Y., Chow, J.C., Watson, J.G., Tie, X.X., Shen, Z.X., Wang, P., An, Z.S., 2012a. Impacts of aerosol compositions on visibility impairment in Xi'an, China. Atmos. Environ. 59, 559–566.

Cao, J.J., Shen, Z.X., Chow, J.C., Watson, J.G., Lee, S.C., Tie, X.X., Ho, K.F., Wang, G.H., Han, Y.M., 2012b. Winter and summer $PM_{2.5}$ chemical compositions in fourteen Chinese cities. J. Air Waste Manage. Assoc. 62, 1214–1226.

Chang, D., Song, Y., Liu, B., 2009. Visibility trends in six megacities in China 1973–2007. Atmos. Res. 94, 161–167.

Che, H., Zhang, X., Li, Y., Zhou, Z., Qu, J.J., 2007. Horizontal visibility trends in China 1981–2005. Geophys. Res. Lett. 34, L24706. http://dx.doi.org/10.1029/2007GL031450.

Che, H., Zhang, X., Li, Y., Zhou, Z., Qu, J.J., Hao, X., 2009. Haze trends over the capital cities of 31 provinces in China, 1981–2005. Theor. Appl. Climatol. 97, 235–242.

Chen, Y., Xie, S.D., 2012. Temporal and spatial visibility trends in the Sichuan Basin, China, 1973 to 2010. Atmos. Res. 112, 25–34.

Chen, L.W.A., Lowenthal, D.H., Watson, J.G., Koracin, D., Kumar, N., Knipping, E.M., Wheeler, N., Craig, K., Reid, S., 2010. Toward effective source apportionment using positive matrix factorization: experiments with simulated $PM_{2.5}$ data. J. Air Waste Manage. Assoc. 60, 43–54.

Cheung, H.C., Wang, T., Baumann, K., Guo, H., 2005. Influence of regional pollution outflow on the concentrations of fine particulate matter and visibility in the coastal area of southern China. Atmos. Environ. 39, 6463–6474.

China Meteorological Administration, 2010. Observation and Forecasting Levels of Haze. QX/T 113-2010 (in Chinese).

Deng, X.J., Tie, X.X., Wu, D., Zhou, X.J., Bi, X.Y., Tan, H.B., Li, F., Jiang, C.L., 2008. Long-term trend of visibility and its characterizations in the Pearl River Delta (PRD) region, China. Atmos. Environ. 42, 1424–1435.

Environmental Protection Agency, 1999. Regional Haze Regulations: Final Rule. 40 CFR Part 51, vol, 64(126). Federal Register, pp. 35714–35774.

Gao, L., Jia, G., Zhang, R., Che, H., Fu, C., Wang, T., Zhang, M., Jiang, H., Yan, P., 2011. Visual range trends in the Yangtze River delta region of China, 1981–2005. J. Air Waste Manage. Assoc. 61, 843–849.

Huang, W., Tan, J., Kan, H., Zhao, N., Song, W., Song, G., Chen, G., Jiang, L., Jiang, C., Chen, R., Chen, B., 2009. Visibility, air quality and daily mortality in Shanghai, China. Sci. Total Environ. 407, 3295–3300.

Hyslop, N.P., 2009. Impaired visibility: the air pollution people see. Atmos. Environ. 43, 182–195.

Jung, J., Lee, H., Kim, Y.J., Liu, X., Zhang, Y., Gu, J., Fan, S., 2009. Aerosol chemistry and the effect of aerosol water content on visibility impairment and radiative forcing in Guangzhou during the 2006 Pearl River Delta campaign. J. Environ. Manag. 90, 3231–3244.

Kim, E., Hopke, P.K., 2004. Source apportionment of fine particles in Washington, DC, utilizing temperature-resolved carbon fractions. J. Air Waste Manag. Assoc. 54, 773–785.

Kim, K.W., Kim, Y.J., Oh, S.J., 2001. Visibility impairment during Yellow Sand periods in the urban atmosphere of Kwangju, Korea. Atmos. Environ. 35, 5157–5167.

Kim, Y.J., Kim, K.W., Kim, S.D., Lee, B.K., Han, J.S., 2006. Fine particulate matter characteristics and its impact on visibility impairment at two urban sites in Korea: Seoul and Incheon. Atmos. Environ. 40, S593–S605.

Koschmieder, H., 1924. Theorie der horizontalen Sichtweite. Beitrage zur Physik der freien Atmosphare, 12, pp. 33–53.

Liu, X.G., Gu, J.W., Li, Y.P., Cheng, Y.F., Qu, Y., Han, T.T., Wang, J.L., Tian, H.Z., Chen, J., Zhang, Y.H., 2013. Increase of aerosol scattering by hygroscopic growth: observation, modeling, and implications on visibility. Atmos. Res. 132–133, 91–101.

Malm, W.C., Day, D.E., 2000. Optical properties of aerosols at Grand Canyon National Park. Atmos. Environ. 34, 3373–3391.

Malm, W.C., Day, D.E., 2001. Estimates of aerosol species scattering characteristics as a function of relative humidity. Atmos. Environ. 35, 2845–2860.

Paatero, P., Tapper, U., 1994. Positive matrix factorization: a non-negative factor model with optimal utilization of error estimates of data values. Environmetrics 5, 111–126.

Tao, J., Ho, K.F., Chen, L., Zhu, L., Han, J., Xu, Z., 2009. Effect of chemical composition of $PM_{2.5}$ on visibility in Guangzhou, China, 2007 spring. Particuology 7, 68–75.

Tao, J., Zhang, L.M., Ho, K.F., Zhang, R.J., Lin, Z.J., Zhang, Z.S., Lin, M., Cao, J.J., Liu, S.X., Wang, G.H., 2014. Impact of $PM_{2.5}$ chemcial compositions on aerosol light scattering in Guangzhou-the largest megacity in South China. Atmos. Res. 135–136, 48–58.

Taylor, S.R., McLennan, S.M., 1985. The continental crust: its composition and evolution. Blackwell, Oxford, p. 315.

Thach, T.Q., Wong, C.M., Chan, K.P., Chau, Y.K., Chung, Y.N., Ou, C.Q., Yang, L., Hedley, A.J., 2010. Daily visibility and mortality: assessment of health benefits from improved visibility in Hong Kong. Environ. Res. 110, 617–623.

Turpin, B.J., Lim, H.J., 2001. Species contributions to $PM_{2.5}$ mass concentrations: revisiting common assumptions for estimating organic mass. Aerosol Sci. Technol. 35, 602–610.

van Oldenborgh, G.J., Yiou, P., Vautard, R., 2010. On the roles of circulation and aerosols in the decline of mist and dense fog in Europe over the last 30 years. Atmos. Chem. Phys. 10, 4597–4609.

Wang, K.C., Dickinson, R.E., Liang, S.L., 2009. Clear sky visibility has decreased over land globally from 1973 to 2007. Science 323, 1468–1470.

Wang, Q., Cao, J., Tao, J., Li, N., Su, X., Chen, L.A., Wang, P., Shen, Z., Liu, S., Dai, W., 2013. Long-term trends in visibility and at Chengdu, China. PLoS ONE 8 (7), e68894. http://dx.doi.org/10.1371/journal.pone.0068894.

Watson, J.G., 2002. Visibility: science and regulation. J. Air Waste Manage. Assoc. 52, 628–713.

Wen, C.C., Yeh, H.H., 2010. Comparative influences of airborne pollutants and meteorological parameters on atmospheric visibility and turbidity. Atmos. Res. 96, 496–509.

Wu, D., 2004. Demographics of the County and City in China. Department of the Ministry of Public Security, China. Qunzhong Press, Beijing, pp. 91–106.

Wu, D., Tie, X., Li, C., Ying, Z., Alexis, K.H.L., Huang, J., Deng, X., Bi, X., 2005. An extremely low visibility event over the Guangzhou region: a case study. Atmos. Environ. 39, 6568–6577.

Xie, S., Liu, Z., Chen, T., Hua, L., 2008. Spatiotemporal variations of ambient PM_{10} source contributions in Beijing in 2004 using positive matrix factorization. Atmos. Chem. Phys. 8, 2701–2716.

Yang, L.X., Wang, D.C., Cheng, S.H., Wang, Z., Zhou, Y., Zhou, X.H., Wang, W.X., 2007. Influence of meteorological conditions and particulate matter on visual range impairment in Jinan, China. Sci. Total Environ. 383, 164–173.

Yuan, C.S., Lee, C.G., Liu, S.H., Chang, J.c., Yuan, C., Yang, H.Y., 2006. Correlation of atmospheric visibility with chemical composition of Kaohsiung aerosols. Atmos. Res. 82, 663–679.

Zhang, Q.H., Zhang, J.P., Xue, H.W., 2010. The challenge of improving visibility in Beijing. Atmos. Chem. Phys. 10, 7821–7827.

Zhao, P., Zhang, X., Xu, X., Zhao, X., 2011. Long-term visibility trends and characteristics in the region of Beijing, Tianjin, and Hebei, China. Atmos. Res. 101, 711–718.